Volume 1
Number 5
December 2024
Pages 857-1068

RSC Pharmaceutics

rsc.li/RSCPharma

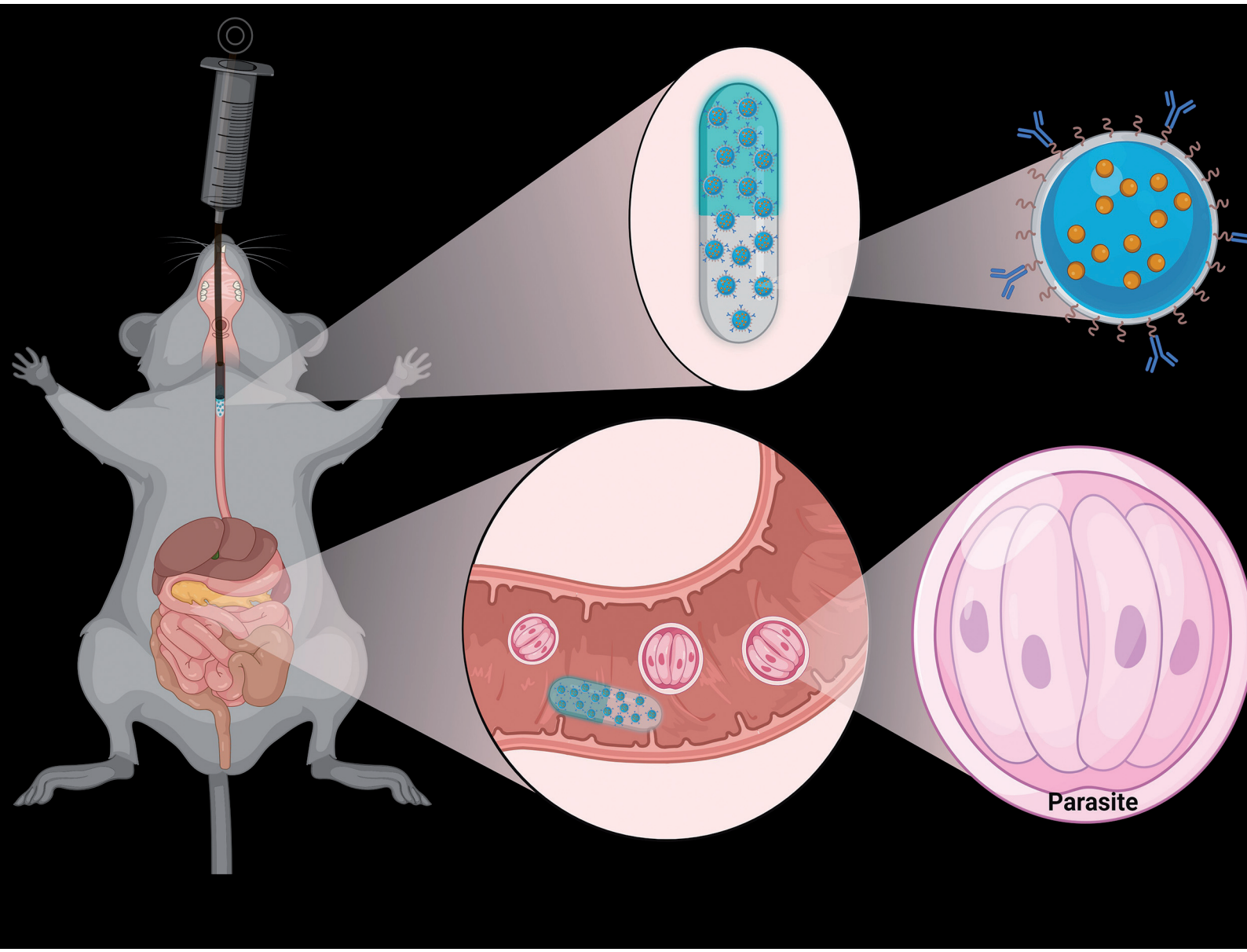

eISSN 2976-8713

ROYAL SOCIETY OF CHEMISTRY

PAPER

Amalendu P. Ranjan, Alejandro Castellanos-Gonzalez, Karen S. Anderson *et al.*
Prodrug nanotherapy demonstrates *in vivo* anticryptosporidial efficacy in a mouse model of chronic *Cryptosporidium* infection

RSC Pharmaceutics

ROYAL SOCIETY OF CHEMISTRY

PAPER

View Article Online
View Journal | View Issue

Check for updates

Cite this: *RSC Pharm.*, 2024, **1**, 963

Prodrug nanotherapy demonstrates *in vivo* anticryptosporidial efficacy in a mouse model of chronic *Cryptosporidium* infection†

Amalendu P. Ranjan, *‡[a] Daniel J. Czyzyk,‡[b] Griselle Martinez-Traverso,[c] Aygul Sadiqova,[c] Margarita Valhondo,[d] Deborah A. Schaefer,[f] Krasimir A. Spasov,[b] William L. Jorgensen, [d] Jamboor K. Vishwanatha,[a] Michael W. Riggs,[f] Alejandro Castellanos-Gonzalez*[c] and Karen S. Anderson *[b,e]

The gastrointestinal disease cryptosporidiosis, caused by the genus *Cryptosporidium*, is a common cause of diarrheal diseases in children, particularly in developing countries and frequently fatal in immunocompromised individuals. *Cryptosporidium hominis* (*Ch*)-specific bifunctional dihydrofolate reductase-thymidylate synthase (DHFR-TS) has been a molecular target for inhibitor design. (*Note that this bifunctional enzyme has also been referred to as TS-DHFR in previous literature since the functional biochemical reaction first involves the conversion of methylene tetrahydrofolate to dihydrofolate at the TS site.*) While nanomolar inhibitors of *Ch* DHFR-TS have been identified at the biochemical level, effective delivery of these compounds to achieve anticryptosporidial activity in cell culture and *in vivo* models of parasite infection remains a major challenge in developing new therapies. Previous studies, using a nanotherapy approach, have shown a promising *Ch* DHFR-TS inhibitor, 906, that can successfully target *Cryptosporidium* parasites in cell culture with nanomolar anticryptosporidial activity. This formulation utilized poly(lactic-*co*-glycolic acid) (PLGA) nanoparticles (NPs) loaded with 906 (NP-906) and conjugated with a *Cryptosporidium* monoclonal antibody (MAb) on the nanoparticle surface to specifically target the glycoprotein GP25–200 in excysting oocysts. However, a limitation for *in vivo* use is antibody susceptibility to gastric acidity. To address this gap, a prodrug diethyl ester form of 906 (MAb-NP-Prodrug) was synthesized that allowed higher compound loading in the MAb-coated PLGA nanoparticles. An oral formulation was prepared by loading lyophilized MAb-NP-Prodrug into gelatin capsules with an enteric coating for gastric stability. Proof-of-concept studies with this oral formulation demonstrated antiparasitic activity in a chronic mouse model of *Cryptosporidium* infection. Efficacy was observed after a low daily dose of 2 × 8 mg kg^{-1} for 5 days, when examined 6 and 20 days postinfection, offering a new avenue of drug delivery to be further explored.

Received 22nd March 2024,
Accepted 16th September 2024

DOI: 10.1039/d4pm00093e

rsc.li/RSCPharma

1. Introduction

Cryptosporidium hominis and *Cryptospordium parvum*, microscopic protozoal parasites, are the primary etiological causes of the diarrheal infection cryptosporidiosis. This illness is contracted through fecal contamination of food and water and can be spread by contact with excrement of infected individuals or ingestion of contaminated recreational water.[1–3] Infection in humans is generally spread through contact with infected individuals' feces or consumption of contaminated recreational water.[4] Recent reports from the Center for Disease Control and Prevention (CDC) indicated that the incidence of cryptosporidiosis is increasing in the United States. While the disease in immunocompetent hosts is often self-limiting, it can be deadly for individuals who are under-nourished, undergoing chemotherapy treatment, or with chronically suppressed

[a]*Department of Microbiology, Immunology and Genetics, College of Biomedical and Translational Sciences, University of North Texas Health Science Center, Fort Worth, TX 76107, USA. E-mail: amalendu.ranjan@unthsc.edu*
[b]*Department of Pharmacology, Yale University School of Medicine, 333 Cedar Street, New Haven, CT 06520, USA. E-mail: karen.anderson@yale.edu; Tel: +1 (203) 785-4526*
[c]*Infectious Disease Division, Department of Internal Medicine, University of Texas Medical Branch, Galveston, TX 77555, USA. E-mail: alcastel@UTMB.edu; Tel: +1 (409) 772-3729*
[d]*Department of Chemistry, Yale University, 225 Prospect Street, PO Box 208107, New Haven, CT 06520, USA*
[e]*Department of Molecular Biophysics and Biochemistry, Yale University School of Medicine, 333 Cedar Street, New Haven, CT 06520, USA*
[f]*School of Animal and Comparative Biomedical Sciences, College of Agriculture and Life Sciences, University of Arizona, Tucson, AZ 85721, USA*

†Electronic supplementary information (ESI) available. See DOI: https://doi.org/10.1039/d4pm00093e

‡These authors contributed equally to this work.

immune systems due to medication or HIV.[4,5] There are limited therapeutic regimens available, including the FDA approved nitazoxanide and paromomycin; however, these agents are not useful for individuals who are immunosuppressed. Therefore, new options for treatment of cryptosporidiosis are badly needed.[6–8]

Recently, several new molecular targets from the genomic information from *Cryptosporidium* sequence data have been described that include inosine monophosphate dehydrogenase (IMPDH), phosphatidylinositol-4-OH kinase, calcium protein kinases, fatty acyl CoA synthetase, methionyl-tRNA synthetase and lysyl-tRNA synthetase.[9–15] Our inhibitor efforts have focused on bifunctional DHFR-TS, a key metabolic enzyme found selectively in several parasitic protozoan species (including *Leishmania*, *Toxoplasma*, *Plasmodium* and *Cryptosporidium*). Most higher eukaryotes, including humans, as well as prokaryotes, express TS and DHFR as two separate enzymes that function independently. The inhibition of either of the catalytic activities of DHFR-TS will result in the shutdown of DNA synthesis and cell death. Genetic studies show that the DHFR-TS gene is essential for parasite survival and is a validated drug target.[16–18] Genomic studies have identified a thymidine kinase in *Cryptosporidium* suggested to arise from horizontal gene transfer which could serve as an alternative pathway for dTMP production when a source of thymidine is provided.[19,20] However, kinetic characterization of the *Cryptosporidium* thymidine kinase has shown that the production of TMP from thymidine is very inefficient (k_{cat}/K_m = 0.00044–0.006 s^{-1} μM^{-1}).[20] In contrast, the *Cryptosporidium* DHFR-TS, which has an extremely fast thymidylate synthase catalytic activity, can utilize dUMP to form TMP (k_{cat}/K_m = 45–80 s^{-1} μM^{-1}), nearly 8000–100 000 times more efficiently.[21,22] Inhibitors of each enzyme have shown anticryptosporidial activity in cell culture and mouse models of *Cryptosporidium* infections.[20,23]

Anti-GP25-200 [2C2] is a monoclonal antibody that recognizes *C. parvum* and *C. hominis*.[24] This antibody has been used as a neutralizing antibody for passive immunization against *Cryptosporidium*.[24] Previous studies in our lab utilized PLGA nanoparticles (NP) conjugated with MAb 2C2.[23] These NPs were used for delivering a model DHFR-TS inhibitor, 2-amino-4-oxo-4,7-dihydro-pyrrolo[2,3-*d*]pyrimidine-methyl-phenyl-L-glutamic acid (compound 906, Fig. 1A). For this proof-of-concept study, we used the MAb C2C, reactive to *C. hominis* and *C. Parvum*, which was commercially available (in the required amounts from Kerafast). However, previous studies have characterized this MAb as a sporozoite antigen.[25] Therefore, C2C reactivity in PVM or other intracellular stages is unclear and needs to be determined in future studies. Alternatively, other MAbs with intracellular localization, that may be available, could be considered as well.

This MAb-NP-906 nanotherapy showed potent inhibition (IC_{50} = 300 nM) in *C. parvum* infected cell culture.[23] *C. parvum* is often used for cell culture and animal studies instead of *C. hominis* due to the ease of collection of oocysts in large numbers from infected ruminants that are primary hosts for *C. parvum*.[26] The sequence alignment of DHFR-TS from *C. parvum* and *C. hominis* reveals nearly identical 98% sequence similarity at the protein level, which allowed us to test the *Ch* DHFR-TS inhibitor in cell culture using *C. parvum* infected cells as well as the mouse model described in the present work. Cell culture studies examined the effect of the MAb alone to inhibit parasite infection.

The current study describes the evaluation of a MAb-NP-Prodrug nanotherapy in a mouse model of chronic *Cryptosporidium* infection and demonstration of antiparasitic activity *in vivo*.

2. Materials and methods

2.1. Prodrug 906 ethyl ester compound preparation

The synthesis of the prodrug 906 ethyl ester (Fig. 1B) was previously reported.[27] This prodrug is a synthetic intermediate in the synthesis of the final active compound 906 (Fig. 1A).

2.2. Nanoparticle formulation

An oil-in-water emulsion solvent evaporation methodology was utilized for nanoparticle preparation in a manner analogous to that reported earlier.[28,29] This procedure involved dissolving

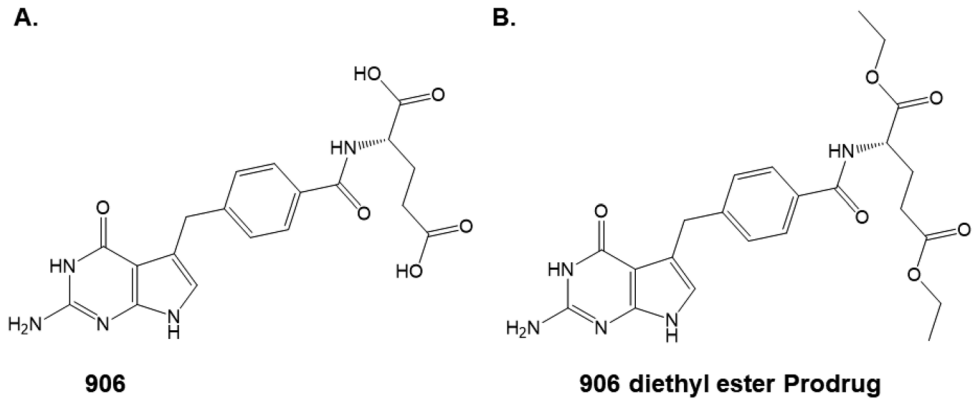

Fig. 1 Chemical modification to improve drug loading. (A) The active compound 906; (B) the diethyl ester of 906 as the prodrug.

50 mg mL^{-1} PLGA 50 : 50 carboxylate end group (iv. 0.55–0.75 dL g^{-1} in hexafluoroisopropanol, HFIP) (Lactel Absorbable Polymers, AL, USA) in 800 μL dichloromethane (DCM). The prodrug (906-ester) (15–25% w/w) was dissolved separately in 200 μL of DCM methanol mixture (8 : 2). This was followed by addition of 200 μL of drug solution to the PLGA solution and vortexing for 30 s. Afterward, 80 μL of methanol was added to achieve a completely homogeneous mixture. This mixture was then transferred to an aqueous solution of 2 mL of 5% poly (vinyl-alcohol) (Sigma, MO, USA) plus 0.5 mg mL^{-1} of bis[sulfosuccinimidyl] suberate (BS3) crosslinker, (ProteoChem, UT, USA). This mixture was sonicated using an ultrasonic processor UP200H system (Hielscher Ultrasonics GmbH, Germany) five times at 40% amplitude for 10 s on ice using continuous mode with 10 s rest. The resulting emulsion was transferred into 10 mL PVA (0.5% w/w) solution for solvent evaporation. Excess solvent was evaporated under continuous magnetic stirring for 4–6 h. These nanoparticles were washed (×3) by centrifugation at 16 000 rcf for 15 min and then resuspended in water. The nanoparticles were stored at 4 °C until used.

2.3. Conjugation of antibody on nanoparticles

Activated PLGA 906-ester nanoparticles and *Cryptosporidium* monoclonal antibody 2C2 against GP25-200 (developed by the Riggs laboratory and now available through Kerafast) were used at a 1 : 60 antibody : NP ratio and suspended in PBS at room temperature for 1 h. Upon completion of the incubation, the excess antibody was removed by centrifugation followed by two washes with PBS to obtain nanoparticles surface-conjugated with the antibody. The nanoparticle pellet was resuspended in PBS for further use.

2.4. Nanoparticle size, polydispersity index and zeta potential measurement

The hydrodynamic particle size, polydispersity index (PDI) and zeta potential of NP-Prodrug and MAb-NP-Prodrug were measured by dynamic light scattering (DLS) utilizing the Zetasizer Nano ZS instrument (Malvern Ltd). Nanoparticles were loaded into a cuvette and measurements were obtained based on the dynamic light scattering of the nanoparticles. For zeta potential, nanoparticles were loaded into a folded capillary cell (Malvern Ltd), and zeta potential measurements were obtained based on the electrophoretic mobility of the nanoparticles.

2.5. Determination of esterified 906 associated with MAb-NP-Prodrug

A known mass of lyophilized MAb-NP-Prodrug was dissolved in DMSO. The samples were sonicated for 5 min and then filtered using an Acrodisc 25 mm syringe filter with a 0.2 μm DMSO safe Nylon membrane (Pall Life Sciences). A 10 μL aliquot of the sample was further dissolved in 89 μL of 180 mM TEAB, pH 8.0, which contained 1 μL of 1 mg mL^{-1} Nevirapine in acetonitrile as an internal standard. The samples were analyzed by HPLC as described in a previous study.[23] The percent encapsulation efficiency (EE) of MAb-NP-Prodrug was calculated using the following expression:[30]

$$\text{EE } \% = \frac{\text{Total drug content in nanoparticles}}{\text{Total drug used in nanopaticle fabrication}} \times 100.$$

The percent drug loading was determined from the total amount of drug extracted from a known weight of nanoparticles using:[30]

$$\text{DL}\% = \frac{\text{Drug content in nanoparticles}}{\text{Weight of nanoparticles}} \times 100.$$

2.6. Filling of the capsules

Gelatin capsules (Size M) (Torpac, New Jersey, USA) were filled with nanoparticles (MAb-NP-Prodrug and Blank NP). These nanoparticles were prepared using the methods described in the Materials and method section.[28,29] The process of filling these capsules is depicted in Fig. 4. Once the capsules were filled and closed manually, we obtained the weight to determine the amount of nanoparticles within the capsules.

2.7. Preparation of the enteric coated capsules

Each gelatin capsule was coated with an enteric polymer (Eudragit L100-55) (Evonik Corporation, New Jersey, USA), by the dip coating method. The coating solution was prepared by dissolving 52 g of enteric polymers in 230 mL of 200% ethanol (Sigma) added slowly under stirring. The stirring was continued until the lumps were completely dissolved and the solution was homogeneous. In order to enhance the elasticity of Eudragit films, 5 mL of propylene glycol (Sigma) as the plasticizer was added to the coating solution and stirred for 10 min. This coating solution was kept overnight (10–16 h) for aging. Next, the nanoparticle-filled gelatin capsules (body side up) were loaded into the slots of the capsule holder. Next, holding the capsule holder at the edges, the entire capsule body along with a portion of the cap was dipped into the coating solution and coated on all sides. This was then allowed to dry for 25 min. The process was repeated to coat the cap side of the capsule as well. This process was repeated twice to ensure uniform coverage of the body with the polymer, especially where the cap overlaps, to ensure the formation of a uniform and thin covering over the capsule. The capsules were allowed to dry at room temperature. These capsules were stored safely to protect from physical damage. The schematic of this process is illustrated in Fig. 4.

2.8. Protein purification, enzyme assay, and data analysis

The biochemical assays to evaluate enzymatic activity with the bifunctional *Ch* DHFR-TS enzyme utilized a protein expression system and purification as previously described.[21] To evaluate the TS activity, a spectrophotometric assay was utilized that monitored the conversion of substrates dUMP and methylene tetrahydrofolate to products dTMP and dihydrofolate at 340 nm ($\Delta\varepsilon$ = 6400 M^{-1} cm^{-1}) at 25 °C.[21] To measure the DHFR catalytic activity, the oxidation of NADPH to NADP was monitored in the presence of dihydrofolate at 340 nm ($\Delta\varepsilon$ =

12 800 M^{-1} cm^{-1}) at 25 °C.[21] The reaction conditions used to determine IC_{50} values for TS and DHFR are described in a previous study.[21] Changes in absorption were determined on a SpectraMax M5 plate reader (Molecular Devices). Data were fitted to an [Inhibitor] *vs.* normalized response with a variable slope equation using GraphPad Prism software (version 7.01).

2.9. *In vitro* cell culture and infection experiments

The *in vitro* cell culture experiments utilized HCT-8 (ATCC) cells that were resuspended in 500 μL of complete medium (RPMI with 10% fetal bovine serum and 1% antibiotic–antimycotic solution penicillin/streptomycin/amphotericin B from Life Technologies, Grand Island, NY). The cells were seeded in 24-well cell culture plates and incubated at 37 °C in 5% CO_2 overnight as previously described.[23] *Cryptosporidium parvum* oocysts (Iowa strain) were obtained from the University of Arizona Cryptosporidium Production Laboratory. For infection experiments, ~1×10^5 oocysts were used per well (diluted in 10 μL). The sporozoites were excysted as follows: the sample with the oocysts was centrifuged at 500*g* for 5 min and the pellet was washed three times with 250 μL of phosphate buffered saline (PBS). After washing, the pellet was resuspended in 50 μL acidic water (pH 2–3) and incubated for 10 min on ice. Excystation medium (complete medium supplemented with 0.8% taurocholate) was then added to the sample and incubated for 1 h at 37 °C. After incubation, excystation (>90%) was confirmed by microscopy. Stock solutions of *Cryptosporidium*-MAb-PLGA-ester 906 (MAb-NP-Prodrug) and PLGA-ester 906 (NP-Prodrug) were diluted with the infection media (RPMI, 1% antibiotic antimycotic solution) to final concentrations of 0, 0.5, 1, and 5 μM. Then, 500 μL of infection media containing the drug was mixed with ~4×10^5 sporozoites for 15 min at 37 °C (5% CO_2) and added to the HCT-8 cells over 2 h. After incubation, the media were removed, and 500 μL of fresh infection media was added. Plates were incubated overnight at 37 °C with 5% CO_2. After incubation, media were removed and cells were washed by adding 500 μL of PBS and then gently removing the supernatant by pipetting. Attached cells were lysed with 350 μL of RLT buffer (from the RNAeasy plus kit, QIAGEN, Valencia, CA) supplemented with β-mercaptoethanol which was added directly to each well. Samples were transferred to 1.5 mL tubes and stored frozen (−20 °C) until subsequent RNA extraction.

2.10. Quantitation of *Cryptosporidium* in HCT-8 cells by qRT-PCR

Quantitation of *Cryptosporidium* parasites per well (24 well plates) was performed by reverse transcription (RT) real-time PCR as previously described.[31] Briefly, RNA was isolated with RNA affinity columns using a commercial kit (QIAGEN RNAeasy plus kit, Valencia, CA). For these experiments, the RNA concentration was determined by spectrophotometry with the Nanodrop 1000 (Thermo Scientific, Wilmington, DE). The parasite numbers were quantified by RT-PCR using the Applied Biosystems® 7500 Real-Time PCR System (Life Technologies, Grand Island, NY). For parasite quantification, each reaction plate included a standard curve created from serial dilutions of RNA derived from a known number of parasites (ESI Fig. 5†). For all the reactions, one step RT-PCR Super Script III was used with ~100 ng of each sample and specific primers for *C. parvum* Cp-F (CAA TCA GCA ACC AAG CTC AA) and Cp-R (TTG TTG AGC AGC AGG TTC AG). Quantitation was normalized to host 18S RNA. For amplification of human 18S, the following primers were used: h18S-F 5′-CCG ATA ACG AAC GAG ACT CTG G-3′ (forward) and h18s-R 5′-TAG GGT AGG CAC ACG CTG AGC C-3′. The conditions for the qRT-PCR were as follows: 5 min 95 °C × 1 and 15 s at 95 °C, 1 min at 65 °C × 40. The specificity of the primers was confirmed by melting curve analysis.

2.11. Animal studies in SCID/Beige mice infected with *Cryptosporidium*

For testing drugs in an *in vivo* model, a *Cryptosporidium* infection mouse model was used (SCID/Beige-mice), as previously described, with some modifications.[32] For testing MAb-NP-Prodrug formulation, 8 week old SCID/Beige mice were used, which underwent a surgical procedure to insert a duodenal catheter. For this model, the catheter was inserted into the duodenum, passed through the abdominal wall, tunneled subcutaneously to the dorsal incision, exteriorized in the scapular region and secured. Then, the drug was administered directly into the duodenum by using the catheter outlet located in the scapular region. The insertion of the catheter and surgical procedures were conducted at Charles River facilities (Hollister, CA). The entire surgical process, including all anesthesia, analgesia, animal preparation and any postoperative care, was approved and monitored by Charles River IACUC. For infection, mice were gavaged with 1×10^6 *C. parvum* oocysts (Iowa strain) contained in 100 μL of PBS as described before.[33] Four days after infection, mice were treated with MAb-NP-Prodrug suspended in 100 μL of PBS or placebo (PBS) *via* a duodenal catheter daily for 5 days. Approximately 25 mg of stool was collected bi-weekly up to day 15 for quantification by qPCR, and all samples were stored at −20 °C until DNA extraction. Experiments were performed in accordance with the Institutional Animal Care and Use Committee of the University of Texas Medical Branch approved protocol.

For testing treatment with enteric coated capsules, 8 week old SCID-Beige mice from Taconic Biosciences (Rensselaer, NY) were used. For these experiments, mice were infected as described before. After 5 days of infection, 2 groups of mice were treated twice a day with enteric coated mini-capsules loaded with lyophilized MAb-NP-Prodrug (group 1, $N = 7$) or enteric capsules loaded only with NPs (group 2, $N = 7$). For dosing mini-capsules, the protocol suggested by Torpac Company was used with some modifications. Briefly, in this experiment, a homemade dosing device was used, as shown in ESI Fig. 4.† Mini-capsules were loaded into the dosing device and then introduced into mice by oral gavage. Stool was collected as described before but collected every day during the treatment and after treatment on days 10, 12, 14, 16, 19 and 20. Stool samples were stored at −20 °C and used for DNA

extraction and parasite quantitation as described above. At the first day and last day of the experiment, the weight of each mouse in treated and untreated groups was determined to evaluate weight gain.

2.12. DNA extraction, RT-PCR analysis and parasite quantitation

To evaluate the anticryptosporidial effects of MAb-NP-Prodrug in catheterized mice, the number of parasites in stool samples obtained at days 0, 8 and 15 was evaluated. For oral enteric coated capsule dose experiments, parasite burden was analyzed using pooled samples to minimize variability due to intermittent oocyst shedding. Samples were pooled as follows: days 1–3 of treatment (pool 1), days 4–6 (pool 2) and days 7–20 after treatment (pool 3).

For all experiments, DNA was extracted from 25 mg (~3 pellets) of stool from each mouse. Extraction and purification of DNA samples were performed using the QIAamp Fast DNA Stool Mini Kit (QIAGEN, Valencia, CA). A standard curve was generated from serial dilutions of DNA extracted from a known number of parasites spiked in mouse stool, and this curve was used to calculate the total number of parasites in each sample (ESI Fig. 5†). The concentration of DNA in samples was determined by UV absorbance spectrophotometry. The samples were stored at −20 °C until subsequent analysis. The parasite burden was determined by qPCR (Applied Biosystems® 7500 Real-Time PCR System) using the iTaq™ Universal SYBR® Green Supermix Kit (Bio-rad, Hercules, CA) with primers for *C. parvum* described above. qPCR was conducted using 2 μL of sample (25 ng) under the following conditions: 20 min 55 °C × 1, 5 min 95 °C × 1, and 15 s at 95 °C, 1 min at 60 °C × 40 cycles. A standard curve was generated from serial dilutions of DNA extracted from a known number of parasites spiked in mouse stool, and this curve was used to calculate the total number of parasites in each sample.

3. Results

The monoclonal antibody (MAb) *Cryptosporidium*-MAb (MAb) used for these studies recognizes the GP25-200 antigen from the parasite as the sporozoites are excysted from the oocysts.[24,25] Our earlier studies initially suggested that the *Cryptosporidium*-specific antibody recognized the *C. parvum* CP2 protein; however, this was not the case.[23] We tested this antibody at concentrations used in the nanoparticle formulation and at 20× and 2500× higher, and there was *no* effect of the MAb alone on parasite infection in cell culture, as shown in ESI Fig. 1.†[23]

In order to test the MAb-NP-906 nanotherapy in a mouse model of *Cryptosporidium* infection, further refinement of the formulation was required since the drug loading efficiency was low (<1%). The lower amount of drug loading restricted the dose of 906 that could be given as an injection to the mice (<1 mg kg^{-1}), whereas other small molecule anticryptosporidial therapeutics are usually given in a dose ranging from 100 mg kg^{-1} to 1000 mg kg^{-1}.[10,31] Therefore, it was necessary to increase the drug loading by at least 10-fold in order to allow a daily dose of 10 mg kg^{-1} to be evaluated in the mouse studies. This required chemical modification of 906 (see Fig. 1).

3.1. A prodrug strategy for optimization of nanoparticle formulation

One of the challenges for an improved formulation was to develop an approach for maintaining a higher concentration of 906 encapsulated within the nanoparticle. The strategy for production of the nanoparticles involves a nanoprecipitation step followed by H_2O washing. Since 906 contains a dicarboxylic acid moiety (Fig. 1A) and is significantly water soluble, a substantial amount of compound is lost during the water wash. Therefore, to decrease the water solubility of compound 906, the diethyl ester prodrug (Fig. 1B) was synthesized as previously described.[23,27,34] This chemical modification would make the molecule more hydrophobic, less water soluble, and therefore more likely to be retained in the nanoparticle. A prodrug strategy, in which the charged carboxylic acid(s) are protected as esters, represents a common approach for drug delivery.[35] This involves transit of the uncharged prodrug across the cell membrane, inside the cell, cleavage by cellular esterases, and release of the active carboxylic acid that interacts with the molecular target protein, in this case, the *Cryptosporidium* DHFR-TS.

Nanoparticles were successfully synthesized using an oil-in-water emulsion solvent evaporation technique in which the prodrug was encapsulated inside the nanoparticles and *Cryptosporidium*-MAb was attached to the outside of the PLGA-based nanoparticles (see Fig. 2, below). The hydrophobic eight-carbon spacer chain of BS3 facilitates entanglement of the antibody in the PVA surfactant layers coated on the nanoparticles. The optimum conjugation of antibodies was achieved by resuspending nanoparticles in phosphate buffer (pH 7.4) and incubation for 1 h at room temperature in a ratio of 1 : 60, antibody to nanoparticles. Nanoparticles with antibody conjugation will also be referred to as MAb-NP-Prodrug. Nanoparticles that have no antibody (prepared similarly to MAb-NP-Prodrug, except for the linkers neutralized with Tris buffer incubation) will be referred to as NP-Prodrug. The initial drug concentration for the nanoformulation was decided at 15% prodrug to PLGA NPs (w/w). This starting concentration yielded an encapsulation efficiency of 52.4 ± 5.0% and a drug loading of 7.1 ± 0.8% (ESI Table 1†). Animal studies warranted higher drug loading; hence, the initial drug concentration was increased to 25% drug-to-polymer ratio for formulating the NPs. This adjusted concentration yielded an encapsulation efficiency of 54.7 ± 5.9% and a drug loading of 12.2 ± 1.3% (ESI Table 1†). It is notable that the chemical modification of 906 to the prodrug provided a >10-fold increase in drug loading that would be required for evaluation in animal studies.

Next, the nanoparticles were characterized for particle size and zeta potential. It was observed that with an antibody

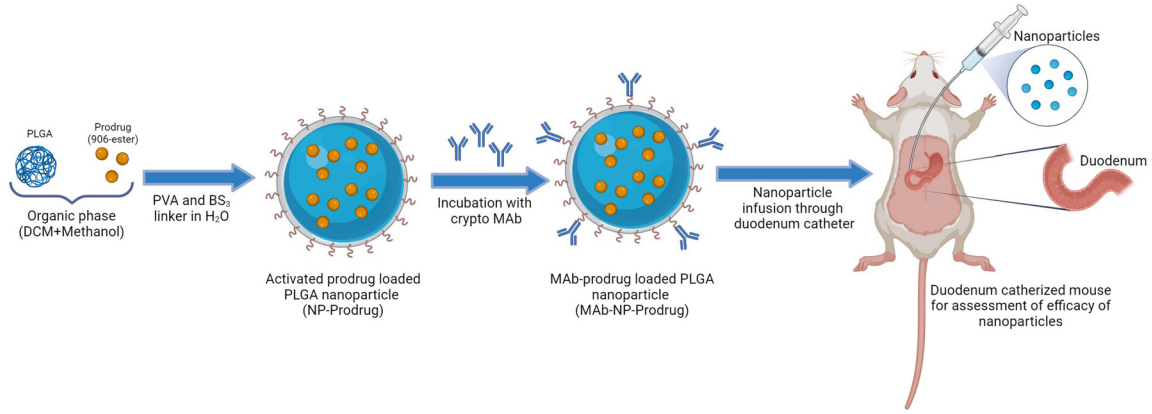

Fig. 2 Schematic diagram representing the experimental design for prodrug nanoformulation and duodenum-specific delivery in mouse.

coating on PLGA nanoparticles, the size of the nanoparticles increased slightly. The hydrodynamic diameters of the NP-Prodrug (mean = 246.6 ± SD 2.85) and MAb-NP-Prodrug (mean = 259.9 ± SD 3.70) were measured by dynamic light scattering. The polydispersity was also calculated for the NP-Prodrug (mean = 0.082 ± SD 0.077) and the MAb-NP-Prodrug (mean = 0.284 ± SD 0.038) (ESI Fig. 2A & B†). The zeta potential of a nanoparticle is a significant parameter as it plays an important role in the cellular interaction of nanoparticles and suspension stability. Results indicated that the zeta potential of nanoparticles shifted towards the positive, from an initial value of −11.6 ± 0.035 mV to −0.627 ± 0.169 mV upon attachment of antibodies to the surface of nanoparticles, a change which can be ascribed to the amphiphilic nature of antibodies (ESI Fig. 2C†).

3.2. Anticryptosporidial activity of prodrug nanotherapy in cell culture

Our earlier biochemical studies with 906 showed a half-maximal inhibitory concentration (IC_{50}) of 0.38 ± 0.04 μM against *Ch*-TS enzyme activity.[34] The anticryptosporidial activity of 906 alone or in nanoparticles in cell culture (half-maximal effective concentration; EC_{50}) required to significantly reduce *C. parvum* infection ranged between 1 and 5 μM on both sporozoite and intracellular forms of the parasite.[34] However, as previously reported, the *Cryptosporidium*-MAb-conjugated 906 NP (MAb-NP-906) delivery strategy improved the therapeutic efficiency for *C. parvum* sporozoites in cell culture (EC_{50} = 100–300 nM range), in agreement with the results at the biochemical level and as noted above, the MAb alone has no effect on parasite infection (ESI Fig. 1†).[23]

The previously determined three-dimensional structure of 906 bound to the active site of the TS domain in ChDHFR-TS revealed key interactions between the γ-carboxylic acid in the compound and the serine 290.[27,34] The chemical modification of 906 to the prodrug was anticipated to decrease the interactions with protein and lower the IC_{50} value at the biochemical level, and this was indeed the case as the IC_{50} for prodrug was determined to be >100 μM and 30 μM for ChTS and ChDHFR, respectively (Table S2†). It was important to establish that chemical modification of 906 to prodrug did not affect the antiparasitic activity in cell culture when loaded into the antibody-coated nanoparticles, MAb-NP-Prodrug. Using the prodrug strategy, the prodrug containing two ethyl esters is expected to be released from nanoparticles in cell culture and hydrolyzed by cellular esterases to the active component, 906. As illustrated in ESI Fig. 3,† the anticryptosporidial activity of the MAb-NP-Prodrug (ESI Fig. 3,† blue bars) is in the 100–300 nM range as was observed in previous experiments with MAb-NP-906 in cell culture and 906 at the biochemical level.[23,34] With NP-Prodrug lacking the *Cryptosporidium* MAb, the EC_{50} is in the 5 μM range (ESI Fig. 3,† red bars), which is consistent with potency similar to the earlier experiments examining NP-906.[23]

3.3. *In vivo* anticryptosporidial efficacy of prodrug nanotherapy in SCID/Beige mice infected with *Cryptosporidium*

The studies described above establish that the prodrug allows 10-fold higher loading of the compound into the antibody-coated nanoparticles and that the MAb-Prodrug-NP formulation retains potent anticryptosporidial activity in cell culture. As a first step toward evaluating efficacy in a mouse model of chronic *Cryptosporidium* infection, a proof-of-concept experiment was designed to examine the effects of the prodrug nanoformulation when delivered directly through a surgically implanted duodenal catheter to the site of parasite infection in the GI tract using a gastric bypass strategy without the confounding factors of metabolism and gastric stability. The experimental design, illustrated in Fig. 2, was implemented in SCID/Beige mice infected with *C. parvum* oocysts.[33]

The treatment regimen is outlined in Fig. 3A. The mice were infected with oocysts, and after 4 days, they were treated with a daily dose of MAb-NP-Prodrug at 10 mg kg^{-1} for 5 days. Stool samples were collected at 0, 8, and 15 days, and parasites were quantified by qRT-PCR. The quantitation for each animal is shown in ESI Table 3.† As shown in Fig. 3B, (▲), 3 out of 5 treated mice showed no detectable parasites at day 8 in the early

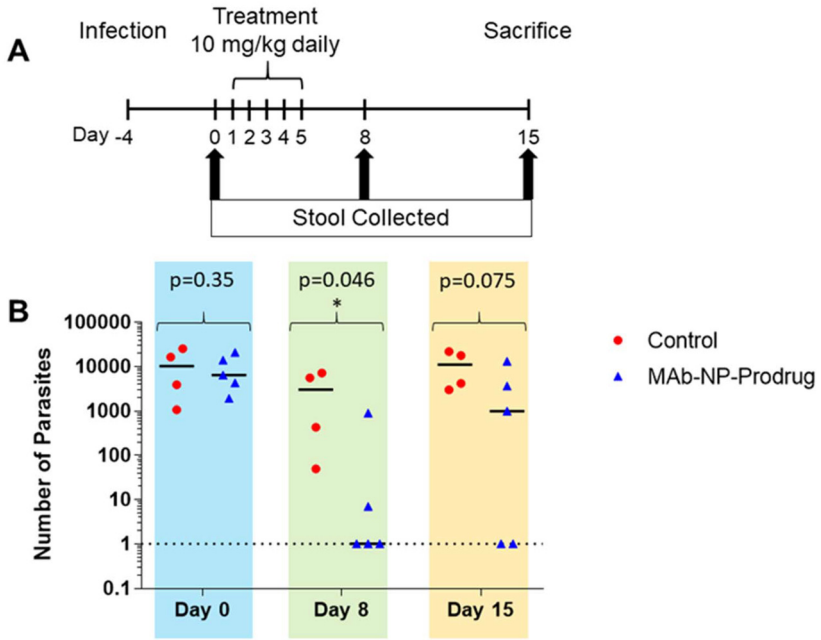

Fig. 3 The effects of MAb-NP-Prodrug in SCID/Beige mice infected with *Cryptosporidium*. Experimental design for infection, drug treatment, and sample analysis for mouse experiments (A). Mice implanted with duodenal catheters were infected orally with 1×10^6 oocysts. After 4 days, mice were treated with MAb-NP-Prodrug (n = 5) or with control, phosphate buffered saline (n = 4) once a day for 5 days at a dose of 10 mg kg^{-1}. Infection was evaluated at days 0, 8 and 15 by quantifying the number of parasites in stools (25 mg) (B). Graph shows untreated mice (●) and treated mice (▲); significance p = 0.045 ($p \leq 0.05$) value day 8 is indicated (*) and day 15 trends toward significant. Data were fit using Student's t-test calculator with two independent means. The experiment was performed in duplicate.

stage of parasite infection. An additional mouse showed a substantial 2 log drop in parasite load. In the later stage of parasite infection, at day 15, 2 out of the 3 mice that originally showed no detectable parasites at day 8 remained cured, while parasite rebound occurred in the 3rd mouse. These results demonstrate promising *in vivo* efficacy of the prodrug nanoformulation.

3.4. Development of an oral prodrug nanoformulation showing *in vivo* anticryptosporidial efficacy

Since the *Cryptosporidium* infection occurs in the GI tract, an ideal drug formulation would need to be stable to gastric acid in the stomach and then released in the duodenum. There have been several successful oral drug delivery studies reported which utilize a capsule coated with an enteric stable polymer that protects the contents of the capsule in the low pH of the stomach, but then dissolves and allows for drug release in the higher pH environment of the duodenal region of the intestine.[4,36,37] An enteric capsule would be required for the MAb-NP-Prodrug to maintain the integrity of the *Cryptosporidium* targeting MAb. The approach of using an enteric coating for successful drug delivery of oral formulations containing antibodies to treat a variety of colon diseases has recently been reported.[4,36–38] A second aspect of developing an oral formulation of the antibody-conjugated PLGA-drug nanoparticles is the requirement that the nanoformulation be in the lyophilized form to facilitate its loading into the enteric coated capsules.[39]

As illustrated in Fig. 4, a lyophilized nanoformulation was prepared and evaluated in *Cryptosporidium*-infected cell culture (top panel). The anticryptosporidial activities of the lyophilized NPs, MAb-NP, NP-Prodrug, and MAb-Prodrug were examined in HCT-8 cell culture infected with *C. parvum* at two different concentrations: 0.1 μM and 1 μM, as shown in Fig. 5A.

The anticryptosporidial activity of NP, MAb-NP, and NP-Prodrug showed no effect on parasite growth at concentrations of 0.1 μM prodrug (blue vertical bars) and 1 μM of prodrug (red vertical bars). Note that NP and MAb-NP do not contain prodrug. Also, with concentrations up to 1 μM, there is no effect on parasite growth for the NP-Prodrug without the MAb. On the other hand, at both concentrations of MAb-NP-Prodrug (0.1 and 1 μM), the level of parasites dropped near or below the detection limit. Importantly, as shown in Fig. 5B, the general host cell toxicity on human HCT-8 cells for each combination was examined in the absence of parasites, and no effects on cell viability were observed even at the very high concentrations (500 μM) of prodrug. These initial studies suggest antiparasitic activity in the 100 nM range and no general cellular toxicity at a concentration of 500 μM. This ratio of efficacy to toxicity suggests a wide therapeutic index of >5000-fold and confirms the nanotherapy approach as an effective, parasitic-specific drug delivery strategy.

Establishing that the lyophilized MAb-NP-Prodrug formulation retained potent anticryptosporidial activity and a wide

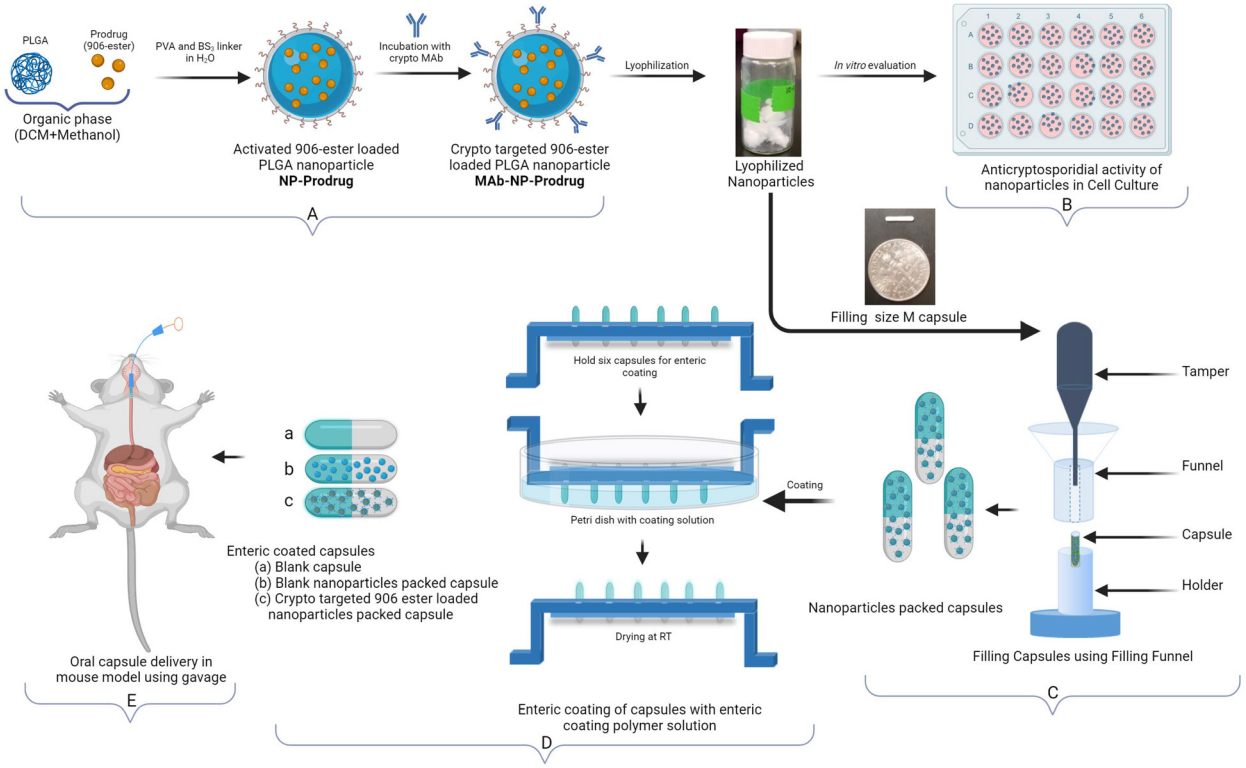

Fig. 4 Schematic diagram representing the experimental design of (A) crypto targeted 906 ester loaded PLGA nanoparticles, (B) *in vitro* evaluation, (C) nanoparticles packing in capsules, (D) enteric coating of capsules, (E) oral delivery of nanoparticle carrying capsules in the mouse model and anticryptosporidial activity testing.

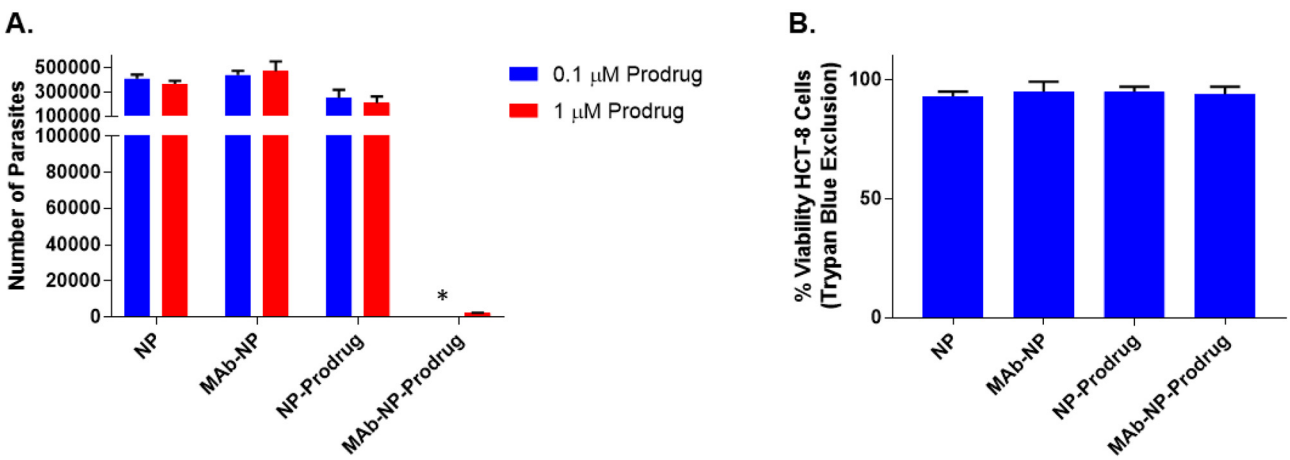

Fig. 5 Evaluation of lyophilized nanoparticle formulations in cell culture for anticryptosporidial activity and general cytotoxicity. (A) Anticryptosporidial activity in cell culture for NP, MAb-NP, NP-Prodrug, and MAb-NP-Prodrug. The concentrations listed, 0.1 μM (blue) and 1 μM (red), refer to the prodrug concentration contained in NPs. Equivalent amounts of nanoparticles were used for NP and MAb-NP, which do not contain prodrug. The anticryptosporidial activity was determined by quantitating the number of parasites (per well) by RT-PCR. (*), below the detection limit of the experiment. The results are shown as the average of 3 independent experiments (bars); ±SD of the means are indicated with vertical bars. (B) HCT-8 cell toxicity for NP, MAb-NP, NP-Prodrug, and MAb-NP-Prodrug at 500 μM prodrug. An equivalent amount of nanoparticles was used for NP and MAb-NP, which do not contain prodrug. The results are shown as the average of 3 independent experiments (bars), ±SD of the means are indicated with vertical bars.

therapeutic window, the lyophilized MAb-NP-Prodrug was then prepared as an oral formulation, as illustrated in Fig. 4 (lower panel). This was accomplished by loading the lyophilized MAb-NP-Prodrug into gelatin capsules designed for mice (see the size of the capsule relative to a dime in the lower panel of Fig. 4). The packed capsules were then coated with Eudragit

L100-55, a polymer which is specially formulated to be acid-stable but dissolve at the slightly basic pH of the duodenal region of the upper intestine.[38]

The treatment schedule of the experiments to examine the oral efficacy of the capsules is shown in Fig. 6A. The mice were infected with parasites, and 4 days after infection, treatment was initiated by dosing the animals with the enteric coated capsules containing NP or MAb-NP-Prodrug, twice daily (2 × 8 mg kg^{-1}). The parasite quantitation for each animal is shown in ESI Table 4.† As shown for each individual animal, examination of the parasite load showed intermittent, cyclical oocyst shedding as is frequently observed in patients with *Cryptosporidium* infections.[40] The parasite burden was analyzed using pooled samples to minimize variability due to intermittent oocyst shedding. Samples were pooled as follows: days 1–3 of treatment (pool 1), days 4–6 (pool 2) and days 7–20 after treatment (pool 3). A significant drop in parasite burden occurred in the MAb-NP-Prodrug group for pool 2 and at the end of the experiment for pool 3 (Fig. 6B). A significant number of animals in pool 2 were cured of the infection and remained cured at the end of the experiment. The body weight was also examined during the course of the experiment. On the first day and last day of the experiment, each mouse was weighed in treated and untreated groups to evaluate weight gain/loss. As shown in Fig. 7, the mice in the treatment group had a significant weight gain relative to the untreated group.

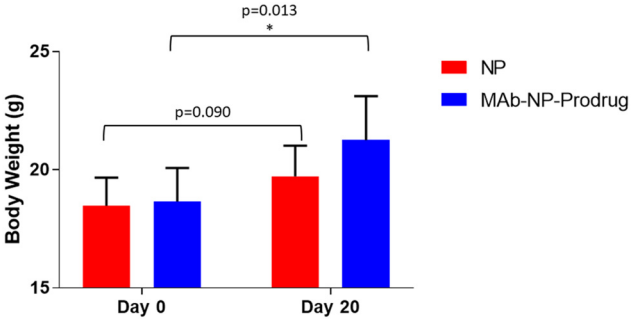

Fig. 7 Comparison of mouse body weights at the beginning of the experiment before parasite infection (day 0) and after infection at the end of the experiment (day 20) after treatment with NPs (red vertical bars) alone or with MAb-NP-Prodrug (blue vertical bars); significance $p = 0.013$ ($p < 0.05$) for MAb-NP-Prodrug is indicated (*).

4. Discussion

The goal of the current study was to design a prodrug nanotherapy strategy for our promising *Ch*DHFR-TS inhibitor 906 that would allow an evaluation of antiparasitic activity in a mouse model of *Cryptosporidium* infection. The key components were using PLGA-based nanoparticles for drug delivery, esterification of 906 to prepare the prodrug which provided a 10-fold increase in the amount of compound in the nanoparticles (NPs), and the attachment of the

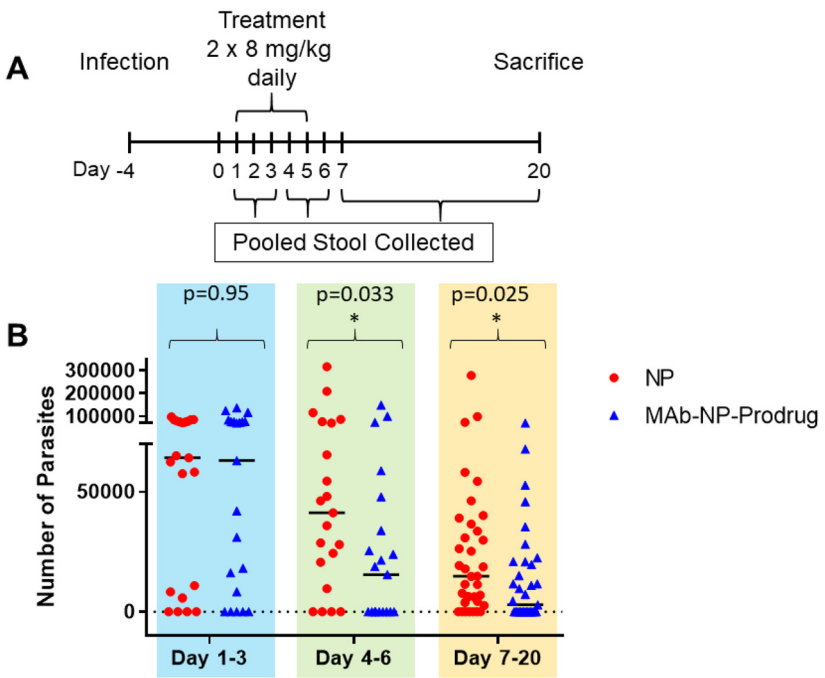

Fig. 6 Oral dosing of enteric coated capsules containing MAb-NP-Prodrug in SCID/Beige mice infected with *Cryptosporidium*. (A) Experimental design for mouse experiments. (B) Mice were infected orally with 1 × 10^6 oocysts. After 4 days, mice were treated with enteric coated capsules containing either MAb-NP-Prodrug ($n = 7$) or NP ($n = 7$), twice a day at 8 mg kg^{-1} for 5 days. Infection was evaluated by quantifying the number of parasites in stools (25 mg), pooled for days 1–3, 4–6, and 7–20, by qRT-PCR. The graph shows untreated mice (▲) and treated mice (●); significance $p = 0.033$, and $p = 0.025$ ($p \leq 0.05$) values for pool days 4–6 and 7–20, respectively, are indicated (*). The experiment was performed in duplicate.

Cryptosporidium-specific MAb, GP-25–200. The optimized MAb-NP-Prodrug nanoformulation maintained nanomolar anticryptosporidial activity in HCT-8 cells infected with *Cryptosporidium*.

An initial proof-of-concept experiment was conducted by examining the *in vivo* anticryptosporidial activity in a chronic SCID/Beige mouse model of *Cryptosporidium* infection. In this experiment, the nanoformulation was delivered directly *via* a duodenal catheter to ensure the likelihood of reaching the GI target site of infection. This complex experimental design allowed an evaluation of the nanoformulation without confounding factors of gastric stability and metabolism. Limitations of this model include the use of a low number of animals, since the model is time-consuming due to the special care that needs to be taken with the catheter. As shown in Fig. 2B, partial protection was demonstrated at a low 10 mg kg^{-1} dose of MAb-NP-Prodrug and 3/5 mice were cleared of infection at day 8 and the remaining mice showed a 2–3 log drop in parasite load. On day 15, it was not unexpected that not all of the mice were cleared of parasites and rebound occurred in one case. These rebounds have been observed with other compounds with anticryptosporidial activity.[33]

In order to have a viable nanoformulation, the next step in further development was to develop an oral formulation of MAb-NP-Prodrug which was protected from gastric acid in the stomach but released at the target site in the intestine where parasite infection with *Cryptosporidium* occurs. A common strategy involves the use of enteric coated capsules which are acid-stable but dissolve in the slightly basic pH of the intestine.[38] Analogous strategies have been utilized for other types of drug-loaded nanoparticles containing conjugated antibodies for other therapeutic indications especially for colon targeted delivery of therapeutics.[4,36,37] To enable the efficient loading of the MAb-NP-Prodrug into gelatin capsules suitable for dosing mice, the nanoformulation was lyophilized. The integrity and anticryptosporidial activity of the lyophilized MAb-NP-Prodrug were maintained in the nanomolar range in HCT-8 cells infected with *Cryptosporidium*. There was no anticryptosporidial activity of the MAb alone, MAb-NP, or NP-Prodrug at these concentrations. Moreover, no general cytotoxicity was noted at concentrations of prodrug up to 500 μM.

An oral formulation was prepared by loading the lyophilized MAb-NP-Prodrug into gelatin capsules for dosing mice followed by enteric coating with polymer (Eudragit L100-55) to provide gastric stability and dissolution in the intestine (see Fig. 4). The efficacy of the oral formulation with enteric coated capsules containing MAb-NP-Prodrug was established by dosing the SCID/Beige mice infected with *C. parvum* at 2 × 8 mg kg^{-1} daily for 5 days (Fig. 6), which showed anticryptosporidial activity relative to those receiving enteric capsules containing blank nanoparticles. An intermittent oocyst shedding was observed, which complicated the evaluation of *in vivo* efficacy when comparing specific days of infection. To overcome this unexpected variation, we analyzed pooled samples of the 3 stages of infection: onset, acute and chronic phases. The chronic and acute phases have been well characterized, so a typical peak can be observed between 4 and 6 days, and then the infection drops between 7 and 21 days.[41] Our results showed significant differences when comparing pooled samples from acute and chronic phases, but not during onset. Although the overall observed protection is partial during the acute and chronic phases, the treatment clearly showed a significant improvement in mouse weight, which is a common parameter to evaluate clinical outcomes from treatments in the mouse model. It cannot be completely ruled out that MAb could have a neutralizing effect and contribute to protection against infection especially at high concentrations. However our *in vitro* experiments[23] demonstrated that MAb alone at the concentrations used here does not reduce infection; thus, the partial protection observed here is most likely related to the prodrug's activity, suggesting that treatment could be optimized to enhance the prodrug's *in vivo* activity. Alternative strategies to improve *in vivo* efficacy include the use of next generation enteric capsules developed to improve the activity of delivered molecules.[43]

It is anticipated that this *Cryptosporidium* antibody-targeting strategy would be broadly applicable for delivery of other anti-cryptosporidial drugs, which could be efficiently encapsulated in PLGA nanoparticles. In addition, the generality of the *Cryptosporidium* antibody conjugation on the surface of nanoparticles would accommodate a range of *Cryptosporidium* antibodies, thus making this a wide-ranging strategy for delivery of anticryptosporidial drugs to target GI infections by increasing the local concentration of the drug around the parasite.

The MAb-NP-Prodrug oral formulation described here is a proof-of-concept study as a new approach for enhancing the drug potency through targeted delivery to the parasite. While drug development efforts are down the road, feasibility is a consideration. The oral efficacy of this lyophilized MAb-NP-Prodrug in the capsule form in a chronic mouse model of *Cryptosporidium* infection represents an important first step. In the current oral MAb-NP-Prodrug formulation, the amount of *Cryptosporidium*-specific monoclonal antibody used is small, a ratio of (1 : 60) relative to nanoparticles. Moreover, based upon the loading efficiency of the prodrug in the NPs, the stoichiometry on a molar basis for MAb to prodrug is also quite small (1 : 1250); thus, smaller quantities of the MAb would be needed.

The landscape for economic feasibility of producing biologics in bulk is changing rapidly, especially for developing countries such as China, India and Africa. There has been an explosion of protein therapeutics worldwide, and major advancements in technologies providing more efficient and less costly production of biologics make such strategies more feasible.[42] For instance, there was a recent report published in *The Lancet Infectious Diseases* journal about a clinical trial at NIH using anti-MERS coronavirus antibodies produced in genetically engineered cattle and other strategies including production of antibodies in plants such as tobacco (plantibodies).[44] In summary, a new approach is offered for selectively targeting *Cryptosporidium* infections and further efforts are underway to demonstrate the broad utility of this strategy as well as enhance the therapeutic efficacy.

Ethical statement

UTMB's Animal resource center (ARC) is AAALAC (Association for the Assessment and Accreditation of Laboratory and Care International) accredited. The ARC follows all standards for AAALAC and IACUC (Institutional Animal Care and Use Committee) compliance and in accordance with the Institutional Animal Care and Use Committee of the University of Texas Medical Branch approved protocol#1907060A.

Author contributions

Amalendu P. Ranjan: writing – review & editing, investigation, validation, methodology, and formal analysis; Daniel J. Czyzyk: writing – original draft, investigation, validation, methodology, and formal analysis; Griselle Martinez-Traverso: investigation; Aygul Sadiqova: investigation; Margarita Valhondo: methodology; Deborah A. Schaefer: methodology; Krasimir A. Spasov: investigation. William L. Jorgensen: methodology. Jamboor K. Vishwanatha: conceptualization; Michael W. Riggs: methodology; Alejandro Castellanos-Gonzalez: conceptualization, investigation, validation, and writing – review & editing; Karen S. Anderson: project administration, conceptualization, funding acquisition, supervision, resources, investigation, validation, and writing – review & editing.

Data availability

The data supporting this article have been included as part of the ESI.†

Conflicts of interest

There are no conflicts to declare.

Acknowledgements

We also wish to thank Dr Firouz Asgarzadeh at Evonik for providing a sample of the Eudragit L100-55 polymer. This work is supported by the National Institutes of Health under Award Numbers (AI083146) to K. S. A., Training Grant (5T32AI007404-23) to D. J. C., and (R21CA194295), (S21MD012472) and (U54MD006882) to J. K. V.

References

1 B. Janssen and J. Snowden, Cryptosporidiosis, in *StatPearls, Treasure Island (FL) ineligible companies. Disclosure: Jessica Snowden declares no relevant financial relationships with ineligible companies*, 2023.

2 U. Ryan, R. Fayer and L. Xiao, Cryptosporidium species in humans and animals: current understanding and research needs, *Parasitology*, 2014, **141**(13), 1667–1685.

3 K. L. Kotloff, J. P. Nataro, W. C. Blackwelder, D. Nasrin, T. H. Farag, S. Panchalingam, Y. Wu, S. O. Sow, D. Sur, R. F. Breiman, A. S. Faruque, A. K. Zaidi, D. Saha, P. L. Alonso, B. Tamboura, D. Sanogo, U. Onwuchekwa, B. Manna, T. Ramamurthy, S. Kanungo, J. B. Ochieng, R. Omore, J. O. Oundo, A. Hossain, S. K. Das, S. Ahmed, S. Qureshi, F. Quadri, R. A. Adegbola, M. Antonio, M. J. Hossain, A. Akinsola, I. Mandomando, T. Nhampossa, S. Acacio, K. Biswas, C. E. O'Reilly, E. D. Mintz, L. Y. Berkeley, K. Muhsen, H. Sommerfelt, R. M. Robins-Browne and M. M. Levine, Burden and aetiology of diarrhoeal disease in infants and young children in developing countries (the Global Enteric Multicenter Study, GEMS): a prospective, case-control study, *Lancet*, 2013, **382**(9888), 209–222.

4 W. Checkley, A. C. White Jr., D. Jaganath, M. J. Arrowood, R. M. Chalmers, X. M. Chen, R. Fayer, J. K. Griffiths, R. L. Guerrant, L. Hedstrom, C. D. Huston, K. L. Kotloff, G. Kang, J. R. Mead, M. Miller, W. A. Petri Jr., J. W. Priest, D. S. Roos, B. Striepen, R. C. Thompson, H. D. Ward, W. A. Van Voorhis, L. Xiao, G. Zhu and E. R. Houpt, A review of the global burden, novel diagnostics, therapeutics, and vaccine targets for cryptosporidium, *Lancet Infect. Dis.*, 2015, **15**(1), 85–94.

5 S. P. O'Hara and X. M. Chen, The cell biology of cryptosporidium infection, *Microbes Infect./Inst. Pasteur*, 2011, **13**(8–9), 721–730.

6 I. Abubakar, S. H. Aliyu, C. Arumugam, N. K. Usman and P. R. Hunter, Treatment of cryptosporidiosis in immunocompromised individuals: systematic review and meta-analysis, *Br. J. Clin. Pharmacol.*, 2007, **63**(4), 387–393.

7 G. Gargala, A. Delaunay, X. Li, P. Brasseur, L. Favennec and J. J. Ballet, Efficacy of nitazoxanide, tizoxanide and tizoxanide glucuronide against Cryptosporidium parvum development in sporozoite-infected HCT-8 enterocytic cells, *J. Antimicrob. Chemother.*, 2000, **46**(1), 57–60.

8 V. P. Kumar, K. M. Frey, Y. Wang, H. K. Jain, A. Gangjee and K. S. Anderson, Substituted pyrrolo[2,3-d]pyrimidines as Cryptosporidium hominis thymidylate synthase inhibitors, *Bioorg. Med. Chem. Lett.*, 2013, **23**(19), 5426–5428.

9 F. S. Buckner, R. M. Ranade, J. R. Gillespie, S. Shibata, M. A. Hulverson, Z. Zhang, W. Huang, R. Choi, C. Verlinde, W. G. J. Hol, A. Ochida, Y. Akao, R. K. M. Choy, W. C. Van Voorhis, S. L. M. Arnold, R. S. Jumani, C. D. Huston and E. Fan, Optimization of Methionyl tRNA-Synthetase Inhibitors for Treatment of Cryptosporidium Infection, *Antimicrob. Agents Chemother.*, 2019, **63**(4), e02061–18.

10 S. K. Gorla, N. N. McNair, G. Yang, S. Gao, M. Hu, V. R. Jala, B. Haribabu, B. Striepen, G. D. Cuny, J. R. Mead and L. Hedstrom, Validation of IMP dehydrogenase inhibitors in a mouse model of cryptosporidiosis, *Antimicrob. Agents Chemother.*, 2014, **58**(3), 1603–1614.

11 F. Guo, H. Zhang, J. M. Fritzler, S. D. Rider Jr., L. Xiang, N. N. McNair, J. R. Mead and G. Zhu, Amelioration of Cryptosporidium parvum infection in vitro and in vivo by targeting parasite fatty acyl-coenzyme A synthetases, *J. Infect. Dis.*, 2014, **209**(8), 1279–1287.

12 J. C. Hanna, V. Corpas-Lopez, S. Seizova, B. L. Colon, R. Bacchetti, G. M. J. Hall, E. M. Sands, L. Robinson, B. Baragana, S. Wyllie and M. C. Pawlowic, Mode of action studies confirm on-target engagement of lysyl-tRNA synthetase inhibitor and lead to new selection marker for Cryptosporidium, *Front. Cell. Infect. Microbiol.*, 2023, **13**, 1236814.

13 U. H. Manjunatha, S. Vinayak, J. A. Zambriski, A. T. Chao, T. Sy, C. G. Noble, G. M. C. Bonamy, R. R. Kondreddi, B. Zou, P. Gedeck, C. F. Brooks, G. T. Herbert, A. Sateriale, J. Tandel, S. Noh, S. B. Lakshminarayana, S. H. Lim, L. B. Goodman, C. Bodenreider, G. Feng, L. Zhang, F. Blasco, J. Wagner, F. J. Leong, B. Striepen and T. T. Diagana, A Cryptosporidium PI(4)K inhibitor is a drug candidate for cryptosporidiosis, *Nature*, 2017, **546**(7658), 376–380.

14 M. G. Nava, J. Szewczyk, J. V. Arrington, T. Alam and S. Vinayak, The Cryptosporidium signaling kinase CDPK5 plays an important role in male gametogenesis and parasite virulence, *Cell Rep.*, 2024, **43**(6), 114263.

15 E. Waldron-Young, W. Wijitrmektong, R. Choi, G. R. Whitman, M. A. Hulverson, R. Charania, A. Keelaghan, L. Li, S. Srinual, S. Nikhar, C. W. McNamara, M. S. Love, L. Huerta, M. A. Bakowski, M. Hu, W. C. Van Voorhis, J. R. Mead and G. D. Cuny, Pyridopyrimidinones as a new chemotype of calcium dependent protein kinase 1 (CDPK1) inhibitors for Cryptosporidium, *Mol. Biochem. Parasitol.*, 2024, **260**, 111637.

16 A. K. Cruz, R. Titus and S. M. Beverley, Plasticity in chromosome number and testing of essential genes in Leishmania by targeting, *Proc. Natl. Acad. Sci. U. S. A.*, 1993, **90**(4), 1599–1603.

17 F. J. Gueiros-Filho and S. M. Beverley, Selection against the dihydrofolate reductase-thymidylate synthase (DHFR-TS) locus as a probe of genetic alterations in Leishmania major, *Mol. Cell. Biol.*, 1996, **16**(10), 5655–5663.

18 K. M. Ivanetich and D. V. Santi, Bifunctional thymidylate synthase-dihydrofolate reductase in protozoa, *FASEB J.*, 1990, **4**, 1594–1597.

19 M. C. Pawlowic, M. Somepalli, A. Sateriale, G. T. Herbert, A. R. Gibson, G. D. Cuny, L. Hedstrom and B. Striepen, Genetic ablation of purine salvage in Cryptosporidium parvum reveals nucleotide uptake from the host cell, *Proc. Natl. Acad. Sci. U. S. A.*, 2019, **116**(42), 21160–21165.

20 X. E. Sun, L. Sharling, M. Muthalagi, D. G. Mudeppa, K. W. Pankiewicz, K. Felczak, P. K. Rathod, J. Mead, B. Striepen and L. Hedstrom, Prodrug activation by Cryptosporidium thymidine kinase, *J. Biol. Chem.*, 2010, **285**(21), 15916–15922.

21 C. E. Atreya and K. S. Anderson, Kinetic characterization of bifunctional thymidylate synthase-dihydrofolate reductase (TS-DHFR) from Cryptosporidium hominis: a paradigm shift for ts activity and channeling behavior, *J. Biol. Chem.*, 2004, **279**(18), 18314–18322.

22 L. T. Doan, W. E. Martucci, M. A. Vargo, C. E. Atreya and K. S. Anderson, Nonconserved residues Ala287 and Ser290 of the Cryptosporidium hominis thymidylate synthase domain facilitate its rapid rate of catalysis, *Biochemistry*, 2007, **46**(28), 8379–8391.

23 A. Mukerjee, P. Iyidogan, A. Castellanos-Gonzalez, J. A. Cisneros, D. Czyzyk, A. P. Ranjan, W. L. Jorgensen, A. C. White Jr., J. K. Vishwanatha and K. S. Anderson, A nanotherapy strategy significantly enhances anticryptosporidial activity of an inhibitor of bifunctional thymidylate synthase-dihydrofolate reductase from Cryptosporidium, *Bioorg. Med. Chem. Lett.*, 2015, **25**(10), 2065–2067.

24 D. A. Schaefer, B. A. Auerbach-Dixon and M. W. Riggs, Characterization and formulation of multiple epitope-specific neutralizing monoclonal antibodies for passive immunization against cryptosporidiosis, *Infect. Immun.*, 2000, **68**(5), 2608–2616.

25 M. W. Riggs, A. L. Stone, P. A. Yount, R. C. Langer, M. J. Arrowood and D. L. Bentley, Protective monoclonal antibody defines a circumsporozoite-like glycoprotein exoantigen of Cryptosporidium parvum sporozoites and merozoites, *J. Immunol.*, 1997, **158**(4), 1787–1795.

26 F. Leoni, C. Amar, G. Nichols, S. Pedraza-Diaz and J. McLauchlin, Genetic analysis of Cryptosporidium from 2414 humans with diarrhoea in England between 1985 and 2000, *J. Med. Microbiol.*, 2006, **55**(Pt 6), 703–707.

27 D. J. Czyzyk, M. Valhondo, W. L. Jorgensen and K. S. Anderson, Understanding the structural basis of species selective, stereospecific inhibition for Cryptosporidium and human thymidylate synthase, *FEBS Lett.*, 2019, **593**(15), 2069–2078.

28 A. S. Gdowski, A. Ranjan, M. R. Sarker and J. K. Vishwanatha, Bone-targeted cabazitaxel nanoparticles for metastatic prostate cancer skeletal lesions and pain, *Nanomedicine*, 2017, **12**(17), 2083–2095.

29 S. I. Thamake, S. L. Raut, Z. Gryczynski, A. P. Ranjan and J. K. Vishwanatha, Alendronate coated poly-lactic-co-glycolic acid (PLGA) nanoparticles for active targeting of metastatic breast cancer, *Biomaterials*, 2012, **33**(29), 7164–7173.

30 A. P. Ranjan, A. Mukerjee, L. Helson and J. K. Vishwanatha, Scale up, optimization and stability analysis of Curcumin C3 complex-loaded nanoparticles for cancer therapy, *J. Nanobiotechnol.*, 2012, **10**, 38.

31 A. Castellanos-Gonzalez, M. M. Cabada, J. Nichols, G. Gomez and A. C. White Jr., Human primary intestinal epithelial cells as an improved in vitro model for Cryptosporidium parvum infection, *Infect. Immun.*, 2013, **81**(6), 1996–2001.

32 P. Xu, G. Widmer, Y. Wang, L. S. Ozaki, J. M. Alves, M. G. Serrano, D. Puiu, P. Manque, D. Akiyoshi, A. J. Mackey, W. R. Pearson, P. H. Dear, A. T. Bankier, D. L. Peterson, M. S. Abrahamsen, V. Kapur, S. Tzipori and G. A. Buck, The genome of Cryptosporidium hominis, *Nature*, 2004, **431**(7012), 1107–1112.

33 A. Castellanos-Gonzalez, H. Sparks, S. Nava, W. Huang, Z. Zhang, K. Rivas, M. A. Hulverson, L. K. Barrett, K. K. Ojo, E. Fan, W. C. Van Voorhis and A. C. White Jr., A Novel Calcium-Dependent Kinase Inhibitor, Bumped Kinase Inhibitor 1517, Cures Cryptosporidiosis in Immunosuppressed Mice, *J. Infect. Dis.*, 2016, **214**(12), 1850–1855.

34 V. P. Kumar, J. A. Ciscernos, K. M. Frey, A. Castellanos-Gonzalez, Y. Wang, A. Gangjee, A. C. White, W. L. Jorgensen and K. S. Anderson, Structural studies provide clues for analog design of specific inhibitors of Cryptosporidium hominis Thymidylate Synthase-Dihydrofolate Reductase, *Bioorg. Med. Chem. Lett.*, 2014, **24**(17), 4158–4161.

35 H. Maag, Prodrugs of Carboxylic Acids, in *Prodrugs: Challenges and Rewards*, ed. Springer, Springer, New York, 2007, pp. 703–792.

36 H. Laroui, E. Viennois, B. Xiao, B. S. Canup, D. Geem, T. L. Denning and D. Merlin, Fab'-bearing siRNA TNFalpha-loaded nanoparticles targeted to colonic macrophages offer an effective therapy for experimental colitis, *J. Controlled Release*, 2014, **186**, 41–53.

37 S. Hua, E. Marks, J. J. Schneider and S. Keely, Advances in oral nano-delivery systems for colon targeted drug delivery in inflammatory bowel disease: selective targeting to diseased versus healthy tissue, *Nanomedicine*, 2015, **11**(5), 1117–1132.

38 N. Reix, P. Guhmann, W. Bietiger, M. Pinget, N. Jeandidier and S. Sigrist, Duodenum-specific drug delivery: in vivo assessment of a pharmaceutically developed enteric-coated capsule for a broad applicability in rat studies, *Int. J. Pharm.*, 2012, **422**(1–2), 338–340.

39 W. Ngamcherdtrakul, T. Sangvanich, M. Reda, S. Gu, D. Bejan and W. Yantasee, Lyophilization and stability of antibody-conjugated mesoporous silica nanoparticle with cationic polymer and PEG for siRNA delivery, *Int. J. Nanomed.*, 2018, **13**, 4015–4027.

40 C. L. Chappell, P. C. Okhuysen, C. R. Sterling and H. L. DuPont, Cryptosporidium parvum: intensity of infection and oocyst excretion patterns in healthy volunteers, *J. Infect. Dis.*, 1996, **173**(1), 232–236.

41 D. Takeuchi, V. C. Jones, M. Kobayashi and F. Suzuki, Cooperative role of macrophages and neutrophils in host Antiprotozoan resistance in mice acutely infected with Cryptosporidium parvum, *Infect. Immun.*, 2008, **76**(8), 3657–3663.

42 G. Büyükköroğlu and B. Şenel, *Engineering monoclonal antibodies: production and applications, in Omics technologies and bio-engineering : towards improving quality of life*, Academic Press, London, United Kingdom; San Diego, CA, United States, Ch. 16, 2018, pp. 353–389.

43 A. Rump, M. L. Kromrey, E. Scheuch, V. Jannin, L. Rehenbrock, M. V. Tzvetkov, W. Weitschies and M. Grimm, In Vivo Evaluation of a Gastro-Resistant HPMC-Based "Next Generation Enteric" Capsule, *Pharmaceutics*, 2022, **14**(10), 1999.

44 J. H. Beigel, J. Voell, P. Kumar, K. Raviprakash, H. Wu, J. A. Jiao, E. Sullivan, T. Luke and R. T. Davey Jr., Safety and tolerability of a novel, polyclonal human anti-MERS coronavirus antibody produced from transchromosomic cattle: a phase 1 randomised, double-blind, single-dose-escalation study, *Lancet Infect. Dis.*, 2018, **18**(4), 410–418.